Nonconforming streamline-diffusion-finite-element-methods for convection-diffusion problems

V. John[1], **J.M. Maubach**[2], **L. Tobiska**[3]

[1] Institut für Analysis und Numerik, Otto-von-Guericke-Universität Magdeburg, PF 4120,
D-39016 Magdeburg, Germany, e-mail: john@mathematik.uni-magdeburg.de
[2] Department of Mathematics and Statistics, University of Pittsburgh, PA 15260, USA,
e-mail: jmaubach@vms.cis.pitt.edu
[3] Institut für Analysis und Numerik, Otto-von-Guericke-Universität Magdeburg, PF 4120,
D-39016 Magdeburg, Germany, e-mail: tobiska@mathematik.uni-magdeburg.de

Summary. We analyze nonconforming finite element approximations of stream-line-diffusion type for solving convection-diffusion problems. Both the theoretical and numerical investigations show that additional jump terms have to be added in the nonconforming case in order to get the same $O(h^{k+1/2})$ order of convergence in L^2 as in the conforming case for convection dominated problems. A rigorous error analysis supported by numerical experiments is given.

Mathematics Subject Classification (1991): 65N30, 65N15

1. Introduction

The streamline-diffusion method (SDFEM) for the solution of convection-diffusion problems has been successfully implemented with the use of conforming finite element spaces. This method was proposed first by Hughes and Brooks in [8] and applied to different problems. Starting with the fundamental work by Nävert [14], it was mainly analyzed by C. Johnson and his co-workers [10], [7], [9]. Nowadays, the convergence properties are well-understood in the conforming case [15], [18], [21], [22], [24].

For computational fluid dynamics applications, finite element methods of the nonconforming type are more attractive then those of conforming type since nonconforming elements more easily fulfill the discrete version of the Babuška-Brezzi condition. Another advantage of using nonconforming finite elements is that the unknowns are only concentrated on the faces which results in a cheap local communication, such that parallel MIMD machines can be used for solving

the large systems of equations, see e.g. [6], [11]. In order to stabilize these methods in the case of moderate and higher Reynolds numbers, several upwind methods (resulting in algebraic systems with M-matrices) have been developed and analyzed in [19], [20], [17], [5],[4]. However, the main drawback of upwind methods is the restricted order of convergence. The SDFEM which is known to combine good stability properties with high accuracy outside interior or boundary layers therefore seems to be a sensible alternative to such upwind schemes. For example, [12] studies a nonconforming SDFEM for the solution of the stationary Navier-Stokes equations but does not pay special attention to the dependency of the error constants on the Reynolds number. In order to study the behaviour of nonconforming SDFEM in more detail we first extend some known conforming convergence results to the nonconforming case. Here, when switching from a conforming to a nonconforming SDFEM, one looses the Galerkin orthogonality and has to consider an additional error, called consistency error. For the standard coercive discrete bilinear form it will be shown that the consistency error is not of optimal order, uniformly with respect to the perturbation parameter ε. As a consequence, the optimal order of convergence is not achieved for smooth solutions. The main objective of this paper is to propose several modified optimal order nonconforming streamline-diffusion finite element discretizations for the solution of the boundary value problem

$$(1) \qquad -\varepsilon \Delta u + b \cdot \nabla u + cu = f \quad \text{in } \Omega, \qquad u = 0 \quad \text{on } \Gamma.$$

These modifications consist of introducing appropriate jump terms into the bilinear form. For these discretizations, theoretical and numerical investigations demonstrate convergence results identical to those for conforming methods. The remainder of this paper is organized as following. First, Sect. 2 introduces necessary notations, and formulates three different nonconforming discretizations of (1). Here, we also describe assumptions on the finite element spaces to be fulfilled. Next, Sect. 3 examines the coerciveness of the bilinear form related to the discretizations and studies convergence properties. Finally, Sect. 4 provides several numerical experiments which corroborate our theory.

2. Notations and preliminaries

Let $\Omega \subset \mathbb{R}^d$, $d = 2, 3$, be a bounded domain with polygonal or polyhedral boundary Γ. We are interested in nonconforming discretizations of the convection diffusion problem

$$(2) \qquad -\varepsilon \Delta u + b \cdot \nabla u + c\,u = f \quad \text{in} \quad \Omega, \qquad u = 0 \quad \text{on} \quad \Gamma$$

under the assumptions that b, c, f are sufficiently smooth functions, and ε is a small positive perturbation parameter. For $V = H_0^1(\Omega)$, the standard weak formulation of the problem (2) reads

Find $u \in V$ such that for all $v \in V$

(3) $$\varepsilon(\nabla u, \nabla v) + (b \cdot \nabla u + c\, u, v) = (f, v),$$

where $(\cdot, \cdot)$ denotes the inner product in $L^2(\Omega)$. Note that under the assumption

(4) $$c - \frac{1}{2}\operatorname{div} b \geq 0$$

there is a unique solution of (3).

   In order to discretize problem (3) a family of triangulations $\mathscr{T}_h$ is constructed which cover the domain $\bar{\Omega}$ with nondegenerate d-simplices K, i.e. triangles if $d = 2$ or tetrahedrons if $d = 3$. Each triangulation is supposed to be compatible, that is, every $(d-1)$ dimensional face of a simplex is shared by at most one other simplex. Let the diameter of a simplex K be given by $h_K = \sup_{x,y \in K} |x - y|$, let ρ_K be the diameter of the largest inscribed ball of K and let h be defined by $h = \max_K h_K$. It is assumed that the family of triangulations is shape regular, which means that there exists a positive constant C, independent of h such that for all triangulations $\mathscr{T}_h$ every simplex $K \in \mathscr{T}_h$ satisfies

$$\frac{h_K}{\rho_K} \leq C.$$

Every $(d-1)$-dimensional face E, which separates two neighbouring d-simplices K_1 and K_2, is associated with a uniquely oriented normal n_E (for definiteness from K_1 to K_2). The jump of a function $v \in V$ across E, denoted by

$$\left[\!\left[v \right]\!\right]_E := v|_{K_1} - v|_{K_2},$$

depends on this unique orientation. The inner products in $L^2(K)$ and $L^2(E)$ will be denoted by $(\cdot, \cdot)_K$ and $< \cdot, \cdot >_E$, respectively. Because this paper focusses on nonconforming finite element methods we have to consider elementwise defined norms and seminorms. For instance

$$\|v\|_h := \left(\sum_K |v|_{1,K}^2 \right)^{1/2}.$$

Each of the studied nonconforming finite element spaces $V_h \not\subset V$ contains a conforming finite element subspace $X_h \subset V$ of piecewise polynomials of degree $k \geq 1$. The simplest example of a nonconforming finite element space V_h is the Crouzeix-Raviart element [3] which consists of piecewise linear functions, with degrees of freedom associated to the midpoint of the edges ($d = 2$) and the barycentre of the faces ($d = 3$), respectively. A systematic introduction to new families of arbitrary high order nonconforming elements can be found in [13]. Note that $\|\cdot\|_h$ is a norm on the conforming subspace X_h but in general only a seminorm on the nonconforming space V_h. We suppose that the following assumptions on the spaces X_h and V_h are fulfilled:

(H1) There is an interpolation operator (see for instance [2]) $I_h : H^2(\Omega) \to X_h \subset V_h$ such that for l, with $0 \le l \le \min(k, 2)$ the estimates

$$(5) \quad |v - I_h v|_{l,K} \quad \le \quad C\, h_K^{m+1-l} \, |v|_{m+1,K} \quad \forall v \in H^{m+1}(K),\ 1 \le m \le k$$

$$(6) \quad \|v - I_h v\|_{0,E} \quad \le \quad C\, h_E^{m+1/2} |v|_{m+1,K} \quad \forall v \in H^{m+1}(K),\ 1 \le m \le k$$

hold.

(H2) For any $(d - 1)$-dimensional face E separating two d-simplices K_1, K_2 we have

$$(7) \qquad \int_E q \,\big[\!\big|v_h\big|\!\big]_E \, ds = 0 \qquad \text{for all } q \in P_{k-1},\ v_h \in V_h,$$

where P_{k-1} denotes the space of polynomials in d variables of degree $k - 1$. Further, for any $(d - 1)$-dimensional face E belonging to the boundary Γ one requires

$$(8) \qquad \int_E q \, v_h \, ds = 0 \qquad \text{for all } q \in P_{k-1},\ v_h \in V_h.$$

Note that (H2), in combination with the homogeneous boundary conditions, guarantees that $\|\cdot\|_h$ is a norm on V_h for $k \ge 1$ using that $\|v_h\|_h = 0$ implies that v_h is constant per element. The restriction to $d = 2$ or $d = 3$ with respect to the dimension guarantees that due to inclusion theorems, see for instance [1], $I_h v$ for $v \in H^2(\Omega) \subset C(\bar{\Omega})$ is well defined in (H1).

With the above conditions in mind we can now formulate different versions of the nonconforming streamline-diffusion finite element method:

Find $u_h \in V_h$ such that for all $v_h \in V_h$

$$(9) \qquad\qquad a_h^i(u_h, v_h) = l_h(v_h), \quad i = 1, 2, 3,$$

where the bilinear forms a_h^i, $i = 1, 2, 3$, and the linear form l_h, respectively, are given by

NSD1 Convective form

$$(10) \qquad a_h^1(u, v) := \begin{cases} \sum_K \left\{ \varepsilon(\nabla u, \nabla v)_K + (b \cdot \nabla u + c\, u, v)_K \right. \\ \left. +(-\varepsilon \Delta u + b \cdot \nabla u + c\, u, \delta_K b \cdot \nabla v)_K \right\} \\ \quad + \sum_E \sigma_E < \big[\!\big|u\big|\!\big]_E, \big[\!\big|v\big|\!\big]_E >_E \end{cases}$$

NSD2 Skew-symmetrized form

$$(11) \quad a_h^2(u, v) := \begin{cases} \sum_K \left\{ \varepsilon(\nabla u, \nabla v)_K + \tfrac{1}{2}[(b \cdot \nabla u, v)_K - (b \cdot \nabla v, u)_K] \right. \\ \left. +(c - \tfrac{1}{2}\mathrm{div}\, b, uv) + (-\varepsilon \Delta u + b \cdot \nabla u + c\, u, \delta_K b \cdot \nabla v)_K \right\} \\ \quad + \sum_E \sigma_E < \big[\!\big|u\big|\!\big]_E, \big[\!\big|v\big|\!\big]_E >_E \end{cases}$$

NSD3 Fully skew-symmetrized form

$$
(12) \quad a_h^3(u,v) := \begin{cases} \sum_K \left\{ \varepsilon(\nabla u, \nabla v)_K + (-\varepsilon \Delta u + b \cdot \nabla u, \delta_K b \cdot \nabla v)_K \right. \\ \left. + \frac{1}{2}[((1 - c\delta_K)b \cdot \nabla u, v)_K - ((1 - c\delta_K)b \cdot \nabla v, u)_K] \right. \\ \left. + (c - \frac{1}{2}\operatorname{div}(b + bc\delta_K), uv)_K \right\} \\ + \sum_E \sigma_E < [\![u]\!]_E, [\![v]\!]_E >_E \end{cases}
$$

and

$$
(13) \qquad l_h(v) := (f, v) + \sum_K (f, \delta_K b \cdot \nabla v)_K .
$$

The size of the positive control parameter δ_K and the nonnegative parameter σ will be determined in the next section. In this section also a discretization error estimate is provided which shows that the solution of (9) converges to the solution of (3) for $h \to 0$ under certain conditions for δ_K. As expected, the convergence rate is influenced by the asymptotic behaviour of σ_E for $h \to 0$. Finally, we note that the three formulations coincide for conforming finite element spaces and differ from each other in the nonconforming case.

3. Error estimates

Let us first study the coerciveness of a_h^i, $i = 1, 2, 3$ on V_h from which we get the unique solvability of the problem (3). To this end, instead of (4), we assume the slightly stronger assumption

$$
(14) \qquad\qquad c - \frac{1}{2}\operatorname{div} b \geq c_0 > 0
$$

and introduce the mesh-dependent norm

$$
|||v||| := \left(\sum_K \left\{ \varepsilon|v|_{1,K}^2 + c_0\|v\|_{0,K}^2 + \delta_K \|b \cdot \nabla v\|_{0,K}^2 \right\} + \sum_E \sigma_E \| [\![v]\!]_E \|_{0,E}^2 \right)^{1/2},
$$

in which the error estimates will be derived. Further, we set

$$
(15) \qquad c_{\max} := \sup_{x \in \Omega} |c(x)| \qquad D_{\max} := \sup_{x \in \Omega} |\operatorname{div}(b(x)c(x))|.
$$

Due to our assumptions of a shape regular mesh, there are constants μ_0, μ_1 independent of K and independent of the triangulation $\mathcal{T}_h$ such that the following local inverse inequalities hold

$$
(16) \qquad \|\Delta v_h\|_{0,K} \quad \leq \quad \mu_1 h_K^{-1} |v_h|_{1,K} \qquad \forall v_h \in V_h, \ \forall K \in \mathcal{T}_h,
$$

$$
(17) \qquad \|v_h|_K\|_{0,E} \quad \leq \quad \mu_0 h_E^{-1/2} \|v_h\|_{0,K} \qquad \forall v_h \in V_h, \ \forall E \subset \partial K.
$$

Remark 1. The proof of the existence of a constant μ_1 under the additional assumption that h/h_K is bounded is given in Theorem 17.2 in [16]. However (17.17) of [16], the scaling properties (17.16) and Theorem 15.2 show that for a regular family of triangulations the inequality (16) still holds. Similarly, we can prove (17).

For each bilinear form a_h^i, $i = 1, 2, 3$ we assume a corresponding assumption (Ai) on the control parameters δ_K and σ_E:

(A1) $0 < \delta_K \leq \min\left(\dfrac{c_0}{4c_{\max}^2}, \dfrac{h_K^2}{2\varepsilon\mu_1^2}\right)$, $\sigma_E \geq \dfrac{3\mu_0^2 \|b\|_{0,\infty,E}^2}{c_0 h_E}$,

(A2) $0 < \delta_K \leq \min\left(\dfrac{c_0}{2c_{\max}^2}, \dfrac{h_K^2}{2\varepsilon\mu_1^2}\right)$, $\sigma_E \geq 0$,

(A3) $0 < \delta_K \leq \min\left(\dfrac{c_0}{2D_{\max}}, \dfrac{h_K^2}{\varepsilon\mu_1^2}\right)$, $\sigma_E \geq 0$.

Lemma 1. *Let the finite element spaces satisfy (H1) and (H2) and the control functions δ_K and σ_E fulfill the assumption (Ai), $i \in \{1, 2, 3\}$. Then, the discrete bilinear form a_h^i is coercive on V_h, i.e.,*

(18) $$a_h^i(v_h, v_h) \geq \frac{1}{2}|||v_h|||^2 \quad \text{for all } v_h \in V_h.$$

Proof. First we consider the bilinear form a_h^1 under the assumption (A1). Using the definition and elementwise integration by parts we obtain

$$
\begin{aligned}
a_h^1(v_h, v_h) &= \sum_K \{\varepsilon|v_h|_{1,K}^2 + (c - \tfrac{1}{2}\operatorname{div} b, v_h^2)_K\} \\
&\quad + \frac{1}{2}\sum_K < b \cdot n, v_h^2 >_{\partial K} + \sum_K \delta_K \|b \cdot \nabla v_h\|_{0,K}^2 \\
&\quad + \sum_K \delta_K(-\varepsilon\Delta v_h + c\, v_h, b \cdot \nabla v_h)_K + \sum_E \sigma_E \|[v_h]\|_{E}\|_{0,E}^2.
\end{aligned}
$$

Since (14) we get

$$
\begin{aligned}
a_h^1(v_h, v_h) &\geq |||v_h|||^2 + \frac{1}{2}\sum_K < b \cdot n, v_h^2 >_{\partial K}
\end{aligned}
$$

(19) $$\quad\quad + \sum_K \delta_K(-\varepsilon\Delta v_h + c\, v_h, b \cdot \nabla v_h)_K,$$

as

$$
\begin{aligned}
|(-\varepsilon\Delta v_h + c\, v_h, \delta_K b \cdot \nabla v_h)_K| &\leq \delta_K \|-\varepsilon\Delta v_h + c\, v_h\|_{0,K} \cdot \|b \cdot \nabla v_h\|_{0,K} \\
&\leq \frac{1}{2}\delta_K \|-\varepsilon\Delta v_h + c\, v_h\|_{0,K}^2 + \frac{1}{2}\delta_K \|b \cdot \nabla v_h\|_{0,K}^2
\end{aligned}
$$

which at its turn leads to

$$
\begin{aligned}
\frac{1}{2}\delta_K \|-\varepsilon\Delta v_h + c\, v_h\|_{0,K}^2 &\leq \delta_K \varepsilon^2 \|\Delta v_h\|_{0,K}^2 + \delta_K \|c\, v_h\|_{0,K}^2 \\
&\leq \delta_K \varepsilon^2 \mu_1^2 h_K^{-2}|v_h|_{1,K}^2 + \delta_K c_{\max}^2 \|v_h\|_{0,K}^2 \\
&\leq \frac{\varepsilon}{2}|v_h|_{1,K}^2 + \frac{c_0}{4}\|v_h\|_{0,K}^2.
\end{aligned}
$$

Thus, the last term in (19) can be absorbed by the first term. Let us now analyze the second term in (19). Considering an extension of v_h outside of Ω by zero, we can also define jumps over an E with $E \subset \Gamma$. In this way we have

$$\frac{1}{2} \sum_K < b \cdot n, v_h^2 >_{\partial K} = \frac{1}{2} \sum_E < b \cdot n_E, \left[\!\left[v_h^2\right]\!\right]_E >_E ,$$

and therefore

$$\left| \frac{1}{2} \sum_K < b \cdot n, v_h^2 >_{\partial K} \right| \leq \frac{1}{2} \sum_E \|b\|_{0,\infty,E} \| \left[\!\left[v_h^2\right]\!\right]_E \|_{0,1,E} .$$

Let us denote for a moment the two triangles having the common face E by $K_{1,E}$ and $K_{2,E}$ and the restriction of v_h onto $K_{i,E}$, $i = 1, 2$, by $v_{h,i}$. In the case $E \subset \Gamma$ we have for one of the $K_{i,E}$ that $v_{h,i} = 0$. Then, for arbitrary $\omega > 0$

$$\begin{aligned}
|\left[\!\left[v_h^2\right]\!\right]_E| &\leq& |\left[\!\left[v_h\right]\!\right]_E| \left(\left.|v_{h,1}|\right|_E + \left.|v_{h,2}|\right|_E\right) \\
&\leq& \omega \left(\left.|v_{h,1}|\right|_E^2 + \left.|v_{h,2}|\right|_E^2\right) + \frac{1}{2\omega} \left[\!\left[v_h\right]\!\right]_E^2
\end{aligned}$$

and by integration over E

$$\| \left[\!\left[v_h^2\right]\!\right]_E \|_{0,1,E} \leq \omega \left(\left.\|v_{h,1}\|\right|_E^2_{0,2,E} + \left.\|v_{h,2}\|\right|_E^2_{0,2,E}\right) + \frac{1}{2\omega} \| \left[\!\left[v_h\right]\!\right]_E \|_{0,2,E}^2 .$$

Using the inequality (17) and setting

$$\omega = \frac{c_0 \, h_E}{6\mu_0^2 \|b\|_{0,\infty,E}}$$

we obtain

$$\begin{aligned}
\| \left[\!\left[v_h^2\right]\!\right]_E \|_{0,1,E} &\leq& \frac{\omega \mu_0^2}{h_E} \|v_h\|_{0,2,K_{1,E} \cup K_{2,E}}^2 + \frac{1}{2\omega} \| \left[\!\left[v_h\right]\!\right]_E \|_{0,2,E}^2 \\
&\leq& \frac{c_0}{6\|b\|_{0,\infty,E}} \|v_h\|_{0,2,K_{1,E} \cup K_{2,E}}^2 + \frac{3\mu_0^2 \|b\|_{0,\infty,E}}{c_0 \, h_E} \| \left[\!\left[v_h\right]\!\right]_E \|_{0,2,E}^2 \\
&\leq& \frac{c_0}{6\|b\|_{0,\infty,E}} \|v_h\|_{0,2,K_{1,E} \cup K_{2,E}}^2 + \frac{\sigma_E}{\|b\|_{0,\infty,E}} \| \left[\!\left[v_h\right]\!\right]_E \|_{0,2,E}^2 .
\end{aligned}$$

Summing up over all faces we have

$$\left| \sum_E < b \cdot n_E, \left[\!\left[v_h^2\right]\!\right]_E >_E \right| \leq \frac{c_0}{4} \|v_h\|_{0,2}^2 + \frac{1}{2} \sum_E \sigma_E \| \left[\!\left[v_h\right]\!\right]_E \|_{0,2,E}^2 ,$$

thus we can absorb this term also into $|||\cdot|||^2$ and (18) holds for $i = 1$.

From the definition of a_h^2 we get immediately

$$a_h^2(v_h, v_h) \geq |||v_h|||^2 + \sum_K (-\varepsilon \Delta v_h + c \, v_h, \delta_K b \cdot \nabla v_h)_K ,$$

thus, using the same technique as above we have (18) for $i = 2$ without assuming a lower bound away from zero for σ_E.

For the fully skew-symmetrized form a_h^3 we get first

$$a_h^3(v_h, v_h) \geq |||v_h|||^2 + \sum_K \delta_K (-\varepsilon \Delta v_h, b \cdot \nabla v_h)_K - \frac{1}{2} \sum_K \delta_K (\operatorname{div}(cb), v_h^2)_K .$$

Assuming (A3) we have similarly to above

$$|\delta_K(-\varepsilon \Delta v_h, b \cdot \nabla v_h)_K| \leq \frac{\delta_K}{2} \|b \cdot \nabla v_h\|_{0,K}^2 + \frac{\varepsilon}{2} |v_h|_{1,K}^2 .$$

Now

$$|\delta_K(\operatorname{div}(cb), v_h^2)_K| \leq \delta_K D_{\max} \|v_h\|_{0,K}^2 \leq \frac{c_0}{2} \|v_h\|_{0,K}^2 ,$$

thus we can absorb both terms into $||| \cdot |||$ and obtain (18). $\quad\square$

Let the exact solution u belong to $H_0^1(\Omega) \cap H^2(\Omega)$ such that

$$-\varepsilon \Delta u + b \cdot \nabla u + c u = f \quad \text{in } L^2(K)$$

for all elements $K \in \mathscr{T}_h$. Multiplying this equation with the test function $v_h + \delta_K b \cdot \nabla v_h$ and integrating it by parts one finds that the exact solution u satisfies

$$(20) \qquad a_h^i(u, v_h) = l_h(v_h) + r_h^i(u, v_h),$$

with

$$(21) \qquad r_h^1(u, v_h) \quad := \quad \sum_K \sum_{E \subset \partial K} < \varepsilon \frac{\partial u}{\partial n}, v_h >_E ,$$

$$(22) \qquad r_h^2(u, v_h) \quad := \quad r_h^1(u, v_h) - \frac{1}{2} \sum_K \sum_{E \subset \partial K} < b \cdot n, u v_h >_E ,$$

$$(23) \qquad r_h^3(u, v_h) \quad := \quad r_h^2(u, v_h) - \frac{1}{2} \sum_K \sum_{E \subset \partial K} \delta_K < c \, b \cdot n, u \, v_h >_E .$$

Note that the term

$$\sum_E \sigma_E < \big[|u|\big]_E, \big[|v_h|\big]_E >_E$$

contained in $a_h(u, v_h)$ made no contribution because $u \in H^2(\Omega)$ implies $\big[|u|\big]_E = 0$ on inner faces and because $u = 0$ at $E \subset \Gamma$. The additional term on the right hand side of (20) emanates from the nonconformity of the method, i.e. v_h can have jumps across an face E. Consequently, instead of the usual Galerkin orthogonality for conforming methods (where $a_h(u - u_h, v_h) = 0$), one here finds

$$a_h^i(u - u_h, v_h) = a_h^i(u, v_h) - a_h^i(u_h, v_h) = r_h^i(u, v_h)$$

and we have additionally to estimate the consistency errors

$$\sup_{v_h \in V_h} \frac{r_h^i(u, v_h)}{|||v_h|||} , \quad i = 1, 2, 3.$$

Now we formulate a technical lemma which is useful to estimate the consistency error of each method. Define $\mathscr{M}_E^\mu : H^1(K) \to P_\mu(E)$ to be the $L^2(E)$ projection onto the space of the restriction to E of all polynomials of degree μ.

Lemma 2. *For any integer m with $0 \le m \le \mu$, there exists a positive constant C such that*

$$
(24) \qquad \left| \int_E \varphi(\psi - \mathscr{M}_E^\mu \psi)\, ds \right| \;\le\; C\, h_E^{m+1} |\varphi|_{1,K} |\psi|_{m+1,K}
$$

$$
(25) \qquad \left| \int_E \varphi(\psi - \mathscr{M}_E^\mu \psi)\, ds \right| \;\le\; C\, h_E^{m+1/2} \|\varphi\|_{0,E} |\psi|_{m+1,K}
$$

for all K with $E \subset \partial K$, $\varphi \in H^1(K)$, and $\psi \in H^{m+1}(K)$.

Proof. The first estimate is already verified in Lemma 3 in [3] but for completeness we repeat the arguments for both estimates which are based on scaling properties and on the application of the Bramble-Hilbert-Lemma.
Let $\hat{K}$ be a reference d-simplex of $\mathbb{R}^d$ and $\hat{E}$ be a $(d-1)$-dimensional face of $\hat{K}$. In order to simplify the notation we assume that E and $\hat{E}$ belong to the same hyperplane $x_d = 0$. Let

$$
F : \hat{x} \to B_K \hat{x} + b_K
$$

denote the standard affine mapping with $K = F(\hat{K})$, $E = F(\hat{E})$ and let B_E be the $(d-1) \times (d-1)$ matrix obtained by crossing out the last row and column of B_K. For any function f defined on K and E, respectively, we let $\hat{f} = f \circ F$. Because of the definition of $\mathscr{M}_E^\mu$ we have

$$
\widehat{\mathscr{M}_E^\mu \psi} = \mathscr{M}_{\hat{E}}^\mu \hat{\psi} \ .
$$

Mapping to the reference element gives

$$
\int_E \varphi(\psi - \mathscr{M}_E^\mu \psi)\, ds = |\det(B_E)| \int_{\hat{E}} \hat{\varphi}(\hat{\psi} - \mathscr{M}_{\hat{E}}^\mu \hat{\psi})\, ds \ .
$$

There are two different ways of estimating the integral on the right hand side of the equation, namely

$$
\left| \int_{\hat{E}} \hat{\varphi}(\hat{\psi} - \mathscr{M}_{\hat{E}}^\mu \hat{\psi})\, ds \right| \;\le\; \|\hat{\varphi}\|_{0,\hat{E}} \|\hat{\psi} - \mathscr{M}_{\hat{E}}^\mu \hat{\psi}\|_{0,\hat{E}}
$$

$$
\le\; C\, \|\hat{\varphi}\|_{0,\hat{E}} |\hat{\psi}|_{m+1,\hat{K}}
$$

or, like in [3],

$$
\left| \int_{\hat{E}} \hat{\varphi}(\hat{\psi} - \mathscr{M}_{\hat{E}}^\mu \hat{\psi})\, ds \right| \;\le\; C\, |\hat{\varphi}|_{1,\hat{K}} \|\hat{\psi} - \mathscr{M}_{\hat{E}}^\mu \hat{\psi}\|_{0,\hat{E}}
$$

$$
\le\; C\, |\hat{\varphi}|_{1,\hat{K}} |\hat{\psi}|_{m+1,\hat{K}} \ .
$$

Applying the affine mapping and standard integral transformations the above estimates result in

$$\left| \int_E \varphi(\psi - \mathscr{M}_E^\mu \psi)\, ds \right| \leq C \left| \frac{\det(B_E)}{\det(B_K)} \right| \|B_K\|^{m+2} \, |\varphi|_{1,K} \, |\psi|_{m+1,K}\,,$$

$$\left| \int_E \varphi(\psi - \mathscr{M}_E^\mu \psi)\, ds \right| \leq C \left| \frac{\det(B_E)}{\det(B_K)} \right|^{1/2} \|B_K\|^{m+1} \, \|\varphi\|_{0,E} \, |\psi|_{m+1,K}\,.$$

Using common estimates for $\det(B_E)$, $\det(B_K)$, $\|B_K\|$ and taking into consideration the regularity of the triangulation we finally get the estimates (24) and (25). $\qquad\square$

Now we formulate our main result.

Theorem 1. *Let the assumptions of Lemma 1 be fulfilled. Moreover, let the exact solution u belong to $H_0^1(\Omega) \cap H^{k+1}(\Omega)$. Then, for the NSD1-method the error estimate*

$$
\begin{aligned}
|||u - u_h||| &\leq C\, h^k \left(\sum_K \lambda_K \, |u|_{k+1,K}^2 \right)^{1/2} \\
&\quad + C\, h^{k+1/2} \left(\sum_E \lambda_E \, |u|_{k+1,K_{1,E} \cup K_{2,E}}^2 \right)^{1/2}.
\end{aligned}
\tag{26}
$$

holds. For the NSD2- and the NSD3-method we have

$$
\begin{aligned}
|||u - u_h||| &\leq C\, h^k \left(\sum_K \lambda_K \, |u|_{k+1,K}^2 \right)^{1/2} \\
&\quad + C\, h^{k-1/2} \left(\sum_E \lambda_E \, |u|_{k+1,K_{1,E} \cup K_{2,E}}^2 \right)^{1/2}.
\end{aligned}
\tag{27}
$$

In both cases λ_K and λ_E are defined by

$$\lambda_K := \varepsilon + h_K^2 + \delta_K + \delta_K^{-1} h_K^2\,, \tag{28}$$

$$\lambda_E := \min\left(\frac{1}{\sigma_E}, \frac{h_E}{\varepsilon}, \frac{1}{h_E} \right)\,. \tag{29}$$

Proof. Put $w_h := I_h u - u_h$. From Lemma 1 we get

$$\frac{1}{2} |||I_h u - u_h|||^2 \leq a_h^i(I_h u - u, w_h) + a_h^i(u - u_h, w_h)\,. \tag{30}$$

The first term on the right hand side of (30) will be estimated by considering each term of $a_h^i(I_h u - u, w_h)$ separately. Setting $w := I_h u - u \in C(\bar{\Omega})$, we begin with a_h^1, its first term is given by

$$
\begin{aligned}
\left| \varepsilon \sum_K (\nabla w, \nabla w_h)_K \right| &\leq \varepsilon \sum_K \|\nabla w\|_{0,K} \cdot \|\nabla w_h\|_{0,K} \\
&\leq C\, \varepsilon^{1/2} \left(\sum_K h_K^{2k} |u|_{k+1,K}^2 \right)^{1/2} |||w_h|||\,.
\end{aligned}
$$

The second term is estimated by using first an elementwise integration by parts

$$(b \cdot \nabla w + c\, w, w_h)_K \;=\; (c - \text{div}\, b, w\, w_h)_K - (b \cdot \nabla w_h, w)_K$$

(31)
$$+ \sum_{E \subset \partial K} < b \cdot n\, w, w_h >_E .$$

The sum over the first term in (31) gives

$$\left| \sum_K (c - \text{div}\, b, w\, w_h)_K \right| \;\leq\; C \sum_K \|w\|_{0,K}\, \|w_h\|_{0,K}$$

$$\leq\; C \left(\sum_K h_K^{2k+2} |u|_{k+1,K}^2 \right)^{1/2} |||w_h||| ,$$

and the sum over the second term can be handled in the following way

$$\left| \sum_K (b \cdot \nabla w_h, w)_K \right| \;\leq\; \sum_K \delta_K^{1/2} \|b \cdot \nabla w_h\|_{0,K}\, \delta_K^{-1/2} \|w\|_{0,K}$$

$$\leq\; C \left(\sum_K \delta_K^{-1} h_K^{2k+2} |u|_{k+1,K}^2 \right)^{1/2} |||w_h||| .$$

The sum over the third term of (31) gives (as $w = 0$ on Γ)

$$\left| \sum_K \sum_{E \subset \partial K} < b \cdot n, w\, w_h >_E \right| \;=\; \left| \sum_E < b \cdot n_E, w\, [\![w_h]\!]_E >_E \right|$$

$$\leq\; C \sum_E \sigma_E^{-1/2} \|w\|_{0,E}\, \sigma_E^{1/2} \| [\![w_h]\!]_E \|_{0,E}$$

$$\leq\; C \left(\sum_E \sigma_E^{-1} h_E^{2k+1} |u|_{k+1,K_{1,E} \cup K_{2,E}}^2 \right)^{1/2} |||w_h||| .$$

Alternatively, we could estimate this term in the following way (using the first estimate in Lemma 2)

$$\left| \sum_K \sum_{E \subset \partial K} < b \cdot n, w\, w_h >_E \right|$$

(32)
$$\leq C \sum_E h_E^{k+1/2} |u|_{k+1, K_{1,E} \cup K_{2,E}}\, h_E^{1/2} |w_h|_{1, K_{1,E} \cup K_{2,E}} ,$$

and estimating the sum over $|w_h|_{1,K}$ by

$$|w_h|_1 \leq \varepsilon^{-1/2} |||w_h||| \quad \text{or} \quad |w_h|_{1,K} \leq C\, h_K^{-1} \|w_h\|_{0,K} \leq C\, h_E^{-1} \|w_h\|_{0,K}.$$

Taking the minimum over these three different possibilities we obtain

$$\left| \sum_K \sum_{E \subset \partial K} < b \cdot n, w\, w_h >_E \right|$$

$$(33) \qquad \leq C \left(\sum_E \min \left(\frac{1}{\sigma_E}, \frac{h_E}{\varepsilon}, \frac{1}{h_E} \right) h_E^{2k+1} |u|_{k+1, K_{1,E} \cup K_{2,E}}^2 \right)^{1/2} |||w_h|||\, .$$

The third term of $a_h^1(w, w_h)$ is bounded by

$$\left| \sum_K (-\varepsilon \Delta w + b \cdot \nabla w + c\, w, \delta_K b \cdot \nabla w_h)_K \right|$$

$$\leq \quad \sum_K \delta_K^{1/2} \left[\varepsilon \|\Delta w\|_{0,K} + C\, h_K^k |u|_{k+1,K} \right] \|\delta_K^{1/2} b \cdot \nabla w_h\|_{0,K}$$

$$\leq \quad C \left(\sum_K (\varepsilon + \delta_K) h_K^{2k} |u|_{k+1,K}^2 \right)^{1/2} |||w_h|||\, .$$

For the last inequality we used the property $\varepsilon \delta_K \leq \mathrm{const}\, h_K^2$ (compare (A1)–(A3)). Finally, for $a_h^1(w, w_h)$ the sum over the jump terms is identical to zero since $\big[|w| \big]_E = \big[|I_h u - u| \big]_E = 0$. Summarizing the estimates for all terms of $a_h^1(w, w_h)$ we get

$$|a_h^i(I_h u - u, w_h)|$$

$$\leq \quad C \left(\sum_K (\varepsilon + h_K^2 + \delta_K + \delta_K^{-1} h_K^2) h_K^{2k} |u|_{k+1,K}^2 \right)^{1/2} |||w_h|||$$

$$(34) \qquad + C \left(\sum_E \min \left(\frac{1}{\sigma_E}, \frac{h_E}{\varepsilon}, \frac{1}{h_E} \right) h_E^{2k+1} |u|_{k+1, K_{1,E} \cup K_{2,E}}^2 \right)^{1/2} |||w_h|||$$

for $i = 1$. In the same way we can estimate also the different terms of $a_h^2(w, w_h)$ and $a_h^3(w, w_h)$. Thus, (34) holds for $i = 1, 2, 3$.

It remains to estimate the consistency errors for which we will apply Lemma 2. Using the assumption (H2) we get for $r_h^1(u, w_h)$

$$r_h^1(u, w_h) \quad = \quad \sum_K \sum_{E \subset \partial K} < \varepsilon \frac{\partial u}{\partial n}, w_h >_E$$

$$= \quad \sum_E < \varepsilon \frac{\partial u}{\partial n_E}, \big[|w_h| \big]_E >_E$$

$$= \quad \sum_E \varepsilon < \frac{\partial u}{\partial n_E} - \mathcal{M}_E^{k-1} \frac{\partial u}{\partial n_E}, \big[|w_h| \big]_E >_E \ .$$

Now, applying the estimate (24) of Lemma 2 with $h_E \leq h_K$ we see that

$$|r_h^1(u, w_h)| \leq C\, \varepsilon^{1/2} \left(\sum_K h_K^{2k} |u|_{k+1,K}^2 \right)^{1/2} |||w_h|||.$$

This gives for NSD1 by applying the triangle inequality

$$
\begin{aligned}
|||u - u_h||| \\
\leq \quad |||w_h||| + |||u - I_h u||| \\
\leq \quad C\,h^k \left(\sum_K \lambda_K |u|_{k+1,K}^2 \right)^{1/2} + C\,h^{k+1/2} \left(\sum_E \lambda_E |u|_{k+1,K_{1,E} \cup K_{2,E}}^2 \right)^{1/2},
\end{aligned}
$$

with λ_K and λ_E defined by (28) and (29), respectively. In order to estimate r_h^2 we start with the identity

$$
\begin{aligned}
r_h^2(u, w_h) - r_h^1(u, w_h) &= -\frac{1}{2} \sum_K \sum_{E \subset \partial K} < b \cdot n, u\, w_h >_E \\
&= -\frac{1}{2} \sum_E < b \cdot n_E\, u, \big[\!\big[w_h \big]\!\big]_E >_E \\
&= -\frac{1}{2} \sum_E < b \cdot n_E\, u - \mathscr{M}_E^{k-1}(b \cdot n_E\, u), \big[\!\big[w_h \big]\!\big]_E >_E .
\end{aligned}
$$

Now applying (24) or (25) we obtain

$$
|r_h^2(u, w_h)| \leq |r_h^1(u, w_h)| + C\,h^{k-1/2} \left(\sum_E \lambda_E |u|_{k+1,K_{1,E} \cup K_{2,E}}^2 \right)^{1/2} |||w_h|||.
$$

For $r_h^3(u, w_h) - r_h^2(u, w_h)$, we find the same estimate by replacing $b \cdot n_E$ by $\delta_K\, c\, b \cdot n_E$. Using the triangle inequality again gives (27). $\quad\square$

Remark 2. Note that in the convection dominated case $\varepsilon \leq h$, Theorem 1 indicates the choice $\delta_K \sim h_K$ and

$$
\sigma_E \sim \begin{cases} h_E^{-1} & \text{for NSD1} \\ h_E^{-2} & \text{for NSD2 and NSD3} \end{cases}
$$

in order to get an 'optimal' error estimate in the L^2-norm. Here, the choice of σ_E for NSD1 results from the coerciveness result (Lemma 1) and for NSD2, NSD3 from the estimation of the consistency error. For these choices the convergence result of conforming SDFEM on general meshes

$$
\|u - u_h\|_0 \leq C\,h^{k+1/2} |u|_{k+1}
$$

is recovered, see [24].

Remark 3. A careful study of the convergence proof shows that in case of setting $\sigma_E = 0$ an analogous result cannot be obtained. The crucial step is to bound

$$
\sum_E < b \cdot n_E\, u\, , \big[\!\big[w_h \big]\!\big]_E >_E
$$

in terms of $|||w_h|||$, when $\sigma = 0$.

4. Numerical results

In this section we demonstrate the numerical behaviour of the proposed discretization methods for some test examples. The boundary value problem (1) is solved on the unit square $\Omega = (0, 1) \times (0, 1)$ using a finite element discretization with nonconforming P1 elements, thus we have $k = 1$. The method NSD3 is well-suited for an application of the parallel finite element method [11] and it produces similar results as NSD2. The streamline diffusion parameter δ_K is chosen to be

$$\delta_K = \begin{cases} 0 & \text{if} \quad \varepsilon > h_K \\ h_K & \text{if} \quad \varepsilon \leq h_K \end{cases} .$$

The error will be measured in the L^2-norm $\| \cdot \|_0$, the element-wise defined H^1-semi-norm $\| \cdot \|_h$ and the streamline-diffusion norm $\| \cdot \|_S$, which latter is given by

$$\|v\|_S = \left(\varepsilon \|v\|_h^2 + c_0 \|v\|_0^2 + \sum_K \delta_K \|b \cdot \nabla v\|_{0,K}^2 \right)^{1/2} .$$
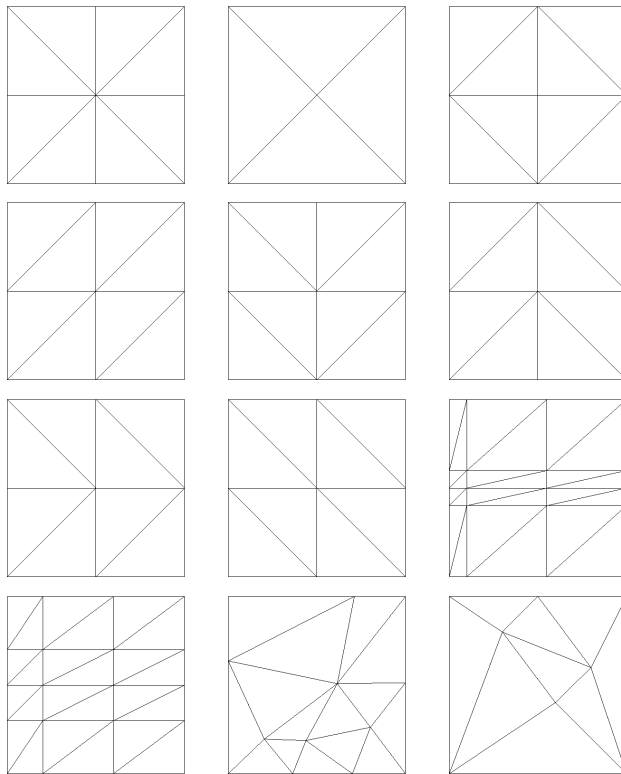
Fig. 1. Various structured and unstructured coarse grids

We solve the discrete problems on a sequence of uniformly refined meshes starting with a coarse grid (level 0). The test calculations have been performed for different types of grids as indicated in Fig. 1. The accuracy of the discetizations has been influenced by the used grid however the rates of convergence in $\| \cdot \|_0$, $\| \cdot \|_h$, and $\| \cdot \|_S$ have been almost independent of the type of the coarse grid. Therefore, we present only the results for Example 1 and 2 using the coarse grid in the upper left corner and for Example 3 using the grid in the upper right corner of Fig. 1. The iterative solver is stopped as soon as the residual of the discrete problem measured in the Euclidean norm is less than 10^{-8}.

Example 1. Smooth polynomial solution.
Let $b = (3, 2)$ and $c = 2$. The right hand side and the boundary conditions are chosen such that

$$u(x, y) = 100(1 - x)^2 x^2 y(1 - 2y)(1 - y)$$

is the exact solution of (1), see Fig. 2.

First we show that for the nonconforming SDFEM without jump terms, i.e. $\sigma_E = 0$, the convergence rates decrease when ε tends to zero. For the numerical tests we have chosen level 6 as the finest level. The convergence rates are computed using the errors on level 5 and 6.

Table 1. Convergence rates for Example 1 and $\sigma_E = 0$

		$\varepsilon = 1$	$\varepsilon = h$	$\varepsilon = h^2$	$\varepsilon = h^4$
NSD1	$\| \cdot \|_0$	1.998	1.751	1.002	0.996
	$\| \cdot \|_h$	0.999	1.178	0.032	-0.043
	$\| \cdot \|_S$	0.999	1.693	1.467	1.158
NSD3	$\| \cdot \|_0$	1.998	1.678	0.056	0.374
	$\| \cdot \|_h$	0.999	0.122	-0.932	-0.695
	$\| \cdot \|_S$	0.999	0.839	0.059	0.189

In order to get an insight in the convergence rates for the range $0 < \varepsilon \le h$ we have chosen ε as a given function of h. In correspondence with Theorem 1 we see that the convergence rate in the $\| \cdot \|_S$-norm for NSD1 reduces for $\varepsilon = h$ to 1.5 and for $\varepsilon = h^2$ to 1. The reduction for NSD3 is much more dramatic, for $\varepsilon = h^2$ it reduces to 0, again as it can be expected from (27). Compared with the well known result for the conforming streamline diffusion method, which gives an error estimate of order 1.5, here we have an additional gap of order 0.5 and 1.0, respectively.

Next we demonstrate the improvements which can be achieved by adding the jump terms to the standard nonconforming SDFEM. In Table 2 and 3 the convergence rates are presented and in Table 4 and 5 the errors. These results reflect the theory given in Sect. 3. Tests with a different direction of the streamlines and a smooth solution gave similar results. Note that for NSD1 the coerciveness of
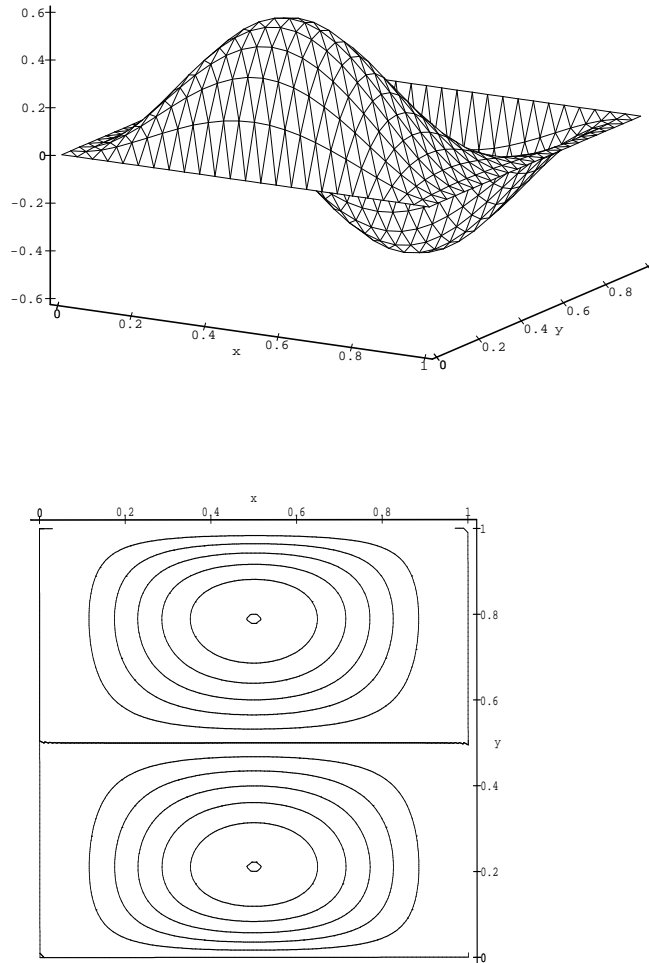
Fig. 2. Exact solution and contour-lines of Example 1

the corresponding bilinear form has been only proven for $\sigma_E \geq C/h$. However the numerical experiments shown in Table 2 and 4 indicate that the method also works for an h independent σ_E. Further, it can be seen that the order of convergence in the L^2-norm is greater than the order in the $\|\cdot\|_S$-norm. This effect of super-convergence has been already reported and studied for the conforming SDFEM in [24]. Moreover, the reduction of convergence rates for NSD3 is one

half less as it could be expected from Theorem 1. However, the absolute error for NSD3 and $\sigma_E = 1$ is much larger than the error for NSD1.

Table 2. Convergence rates of NSD1 for Example 1

		$\varepsilon = h$	$\varepsilon = h^2$	$\varepsilon = h^4$
$\sigma_E = 1$	$\|\cdot\|_0$	1.751	2.002	1.978
	$\|\cdot\|_h$	1.188	0.946	0.986
	$\|\cdot\|_S$	1.696	1.502	1.500
$\sigma_E = 1/h$	$\|\cdot\|_0$	1.752	1.987	1.945
	$\|\cdot\|_h$	1.086	0.973	0.986
	$\|\cdot\|_S$	1.653	1.478	1.477

Table 3. Convergence rates of NSD3 for Example 1

		$\varepsilon = h$	$\varepsilon = h^2$	$\varepsilon = h^4$
$\sigma_E = 1$	$\|\cdot\|_0$	1.692	0.914	1.002
	$\|\cdot\|_h$	0.144	-0.070	0.024
	$\|\cdot\|_S$	0.905	0.975	1.041
$\sigma_E = 1/h$	$\|\cdot\|_0$	1.752	2.022	1.971
	$\|\cdot\|_h$	1.074	0.979	0.983
	$\|\cdot\|_S$	1.646	1.477	1.475

Table 4. Errors for Example 1 and NSD1

		$\varepsilon = h$	$\varepsilon = h^2$	$\varepsilon = h^4$
$\sigma_E = 1$	$\|\cdot\|_0$	.19-2	.70-4	.76-4
	$\|\cdot\|_h$	.39-1	.41-1	.42-1
	$\|\cdot\|_S$	.10-1	.77-2	.77-2
$\sigma_E = 1/h$	$\|\cdot\|_0$	.19-2	.88-4	.93-4
	$\|\cdot\|_h$	.47-1	.45-1	.45-1
	$\|\cdot\|_S$	.11-1	.84-2	.84-2

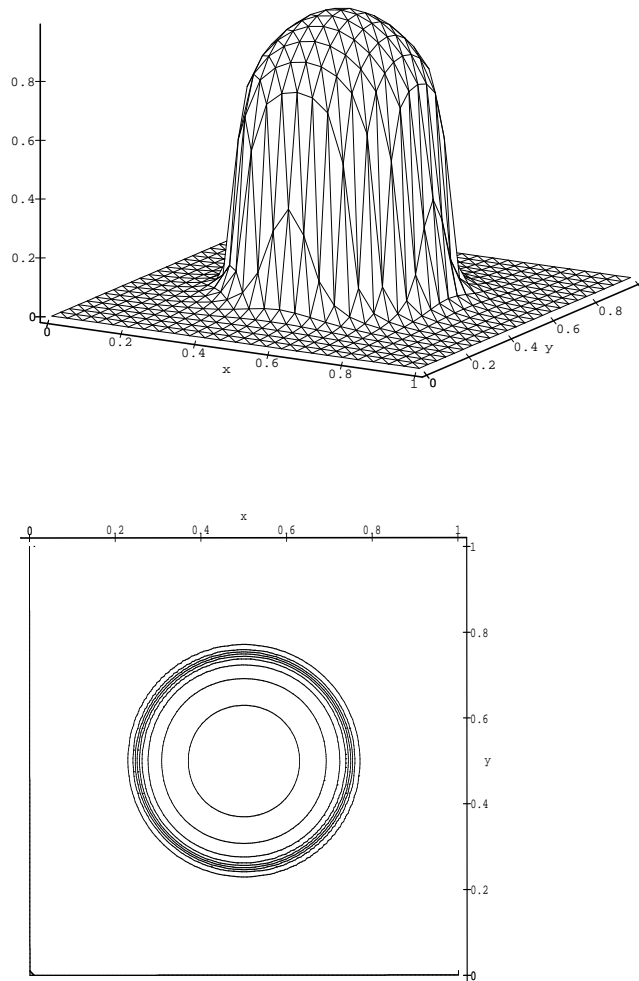**Table 5.** Errors for Example 1 and NSD3

		$\varepsilon = h$	$\varepsilon = h^2$	$\varepsilon = h^4$
$\sigma_E = 1$	$\|\cdot\|_0$	.20-2	.28-2	.30-2
	$\|\cdot\|_h$	.20+0	.14+1	.15+1
	$\|\cdot\|_S$	.26-1	.21-1	.14-1
$\sigma_E = 1/h$	$\|\cdot\|_0$	.19-2	.90-4	.94-4
	$\|\cdot\|_h$	.49-1	.48-1	.48-1
	$\|\cdot\|_S$	.11-1	.85-2	.84-2

Now we will discuss two examples of solutions with layers.

Example 2. Circular internal layer.
Let $b = (2, 3)$ and $c = 2$. The right hand side and the boundary conditions are chosen such that

$$u(x, y) = 16x(1 - x)y(1 - y) \left\{ \frac{1}{2} + \frac{\arctan[200(r_0^2 - (x - x_0)^2 - (y - y_0)^2)]}{\pi} \right\}$$

Fig. 3. Exact solution and contour-lines of Example 2

with $x_0 = y_0 = 0.5$ and $r_0 = 0.25$ is the exact solution of (1), shown in Fig. 3.

Table 6 shows the convergence rates for $\varepsilon = 10^{-4}$ using NSD1 and NSD2 with $\sigma_E = 1$ which are predicted by the theory. The order of convergence is calculated by using the errors of the last two levels. Analogous to Example 1 the convergence rates and the errors of the method NSD1 using $\sigma = 1$ are much better than for NSD2, compare Table 6 with Tables 2–5. This coincides with the
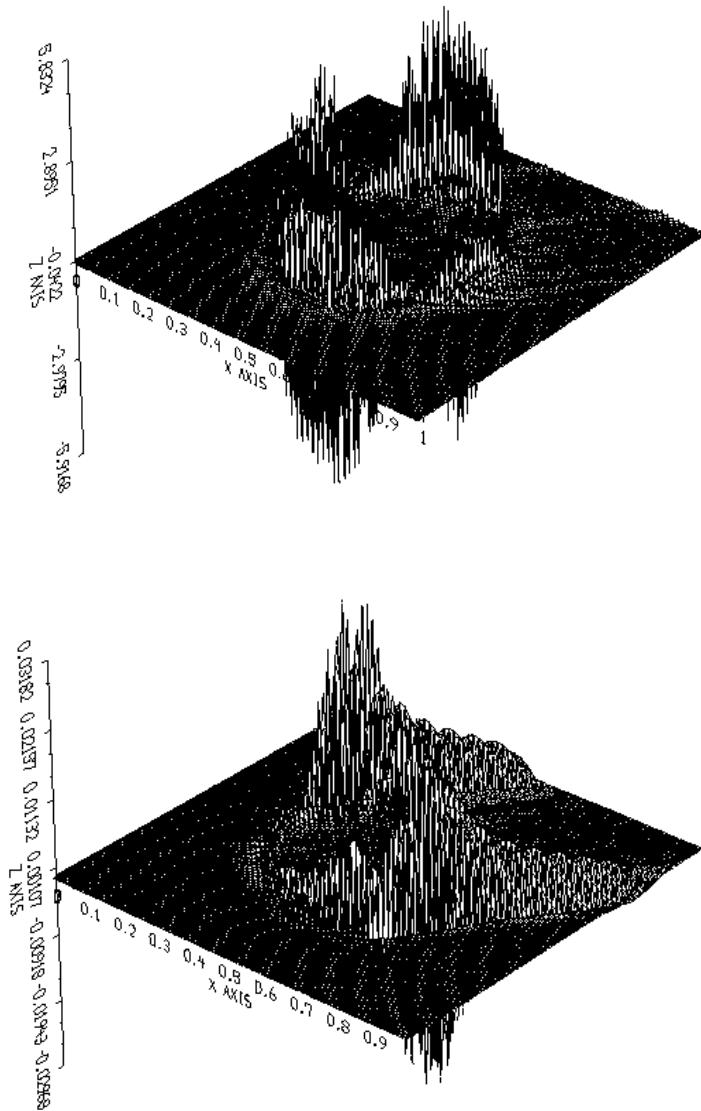
Fig. 4. Error using $\sigma_E = 0$ (upper) and $\sigma_E = 1/h$ (lower), Example 2

theoretical results of Theorem 1. As in Example 1, the choice $\sigma = 1/h$ leads to the nearly the same results for both methods, compare Table 7 with Tables 2–5.

For solving the corresponding linear equations we applied a multi–grid method. L^2–projections have been used for restriction and prolongation and an ILU_β–smoother has been chosen, see e.g. [23]. With this smoother also the systems on the coarse grid has been solved. In Table 8 we present the number

Table 6. Convergence behaviour of Example 2 for NSD1 (left), NSD2 (right) and $\sigma_E = 1$

level	$\|\cdot\|_0$	$\|\cdot\|_h$	$\|\cdot\|_S$	$\|\cdot\|_0$	$\|\cdot\|_h$	$\|\cdot\|_S$
2	.108+0	.314+1	.138+1	.108+0	.299+1	.137+1
3	.717-1	.369+1	.108+1	.809-1	.329+1	.108+1
4	.307-1	.249+1	.466+0	.421-1	.341+1	.472+0
5	.983-2	.124+1	.202+0	.192-1	.241+1	.208+0
6	.283-2	.577+0	.754-1	.978-2	.197+1	.833-1
7	.773-3	.259+0	.271-1	.521-2	.179+1	.368-1
order	1.872	1.156	1.476	.909	.138	1.179

Table 7. Convergence behaviour of Example 2 for NSD1 (left), NSD2 (right) and $\sigma_E = 1/h$

level	$\|\cdot\|_0$	$\|\cdot\|_h$	$\|\cdot\|_S$	$\|\cdot\|_0$	$\|\cdot\|_h$	$\|\cdot\|_S$
2	.923-1	.216+1	.140+1	.936-1	.217+1	.140+1
3	.605-1	.263+1	.111+1	.613-1	.265+1	.111+1
4	.307-1	.176+1	.506+0	.310-1	.177+1	.507+0
5	.145-1	.127+1	.247+0	.146-1	.127+1	.247+0
6	.687-2	.815+0	.113+0	.691-2	.816+0	.113+0
7	.266-2	.448+0	.493-1	.268-2	.449+0	.493-1
order	1.369	.863	1.197	1.366	.862	1.197

Table 8. Number of multi–grid V–cycles and convergence rates. Example 2 for NSD1 and $\sigma_E = 1$ (left), NSD1 and $\sigma_E = 1/h$ (right)

level	cycles	rate	cycles	rate
2	19	.34	14	.22
3	19	.35	36	.58
4	24	.45	117	.85
5	24	.47	277	.94
6	20	.43	587	.97
7	17	.40	1101	.99

Table 9. Convergence behaviour outside the layers of Example 3 using NSD1, $\varepsilon = 10^{-6}, \sigma_E = 0$ (left) and $\sigma_E = 1$ (right)

level	$\|\cdot\|_0$	$\|\cdot\|_h$	$\|\cdot\|_S$	$\|\cdot\|_0$	$\|\cdot\|_h$	$\|\cdot\|_S$
3	.799-3	.635-1	.212-2	.151-3	.943-2	.216-2
4	.358-3	.605-1	.454-3	.303-4	.349-2	.443-3
5	.292-4	.862-2	.262-3	.920-5	.231-2	.267-3
6	.218-5	.880-3	.536-4	.197-5	.858-3	.541-4
7	.663-6	.705-3	.327-4	.574-6	.575-3	.333-4
order	2.730	1.806	1.501	2.001	1.003	1.502

of multi–grid V–cycles and the convergence rates for solving Example 2 using NSD1 and $\sigma_E = 1$ and $\sigma_E = 1/h$, respectively. The results suggest that for $\sigma_E = 1/h$ the condition number of the system matrix is very bad and strongly depends on h. Thus, one should use $\sigma_E = 1$ for computations.

In Fig. 4 errors of computed solutions, plotted as nonconforming functions, are presented. The different solution quality of the method NSD1 without ($\sigma_E = 0$) and with ($\sigma_E = 1/h$) the jump terms can be seen evidently (note the different scaling of the z-axes of the plots). Applying the nonconforming SDFEM
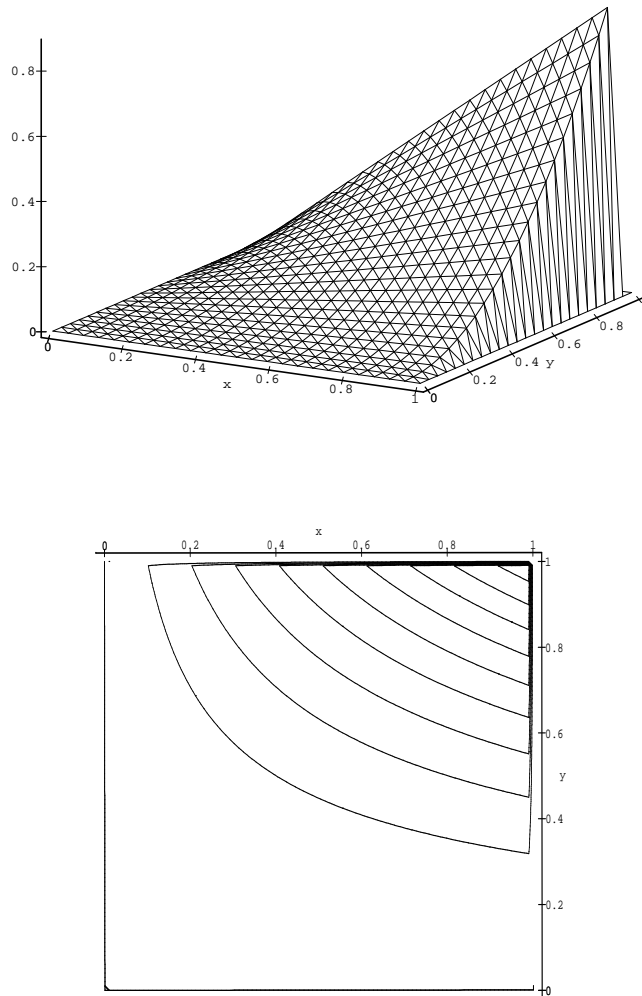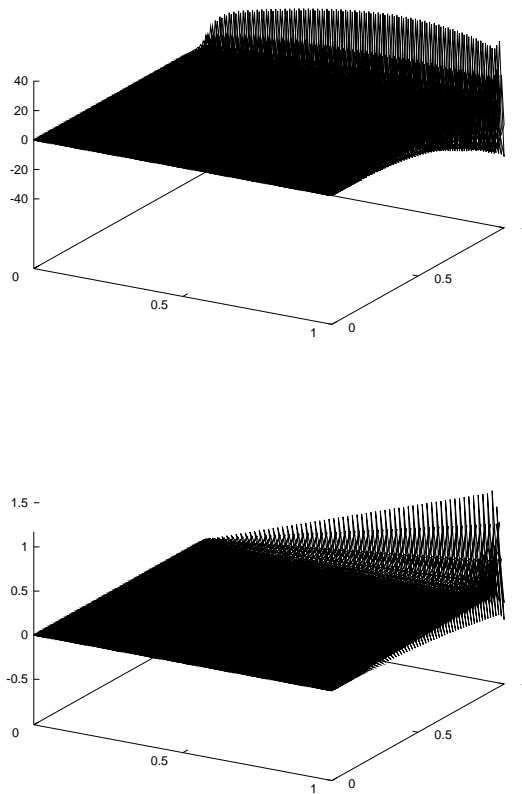
Fig. 5. Exact solution and contour-lines of Example 3

with jump terms the heavy oscillations of the result without the jump terms are considerably damped.

Example 3. Layers at the outflow part of the boundary.

Let $b = (2, 3)$, $c = 1$ the boundary conditions and the right hand side such that

Fig. 6. Errors on level 5 of Example 3 using $\sigma_E = 0$ (upper) and $\sigma_E = 1$ (lower)

$$u(x, y, \varepsilon) \;=\; xy^2 - y^2 \exp\left(\frac{2(x-1)}{\varepsilon}\right) - x \exp\left(\frac{3(y-1)}{\varepsilon}\right)$$
$$+ \exp\left(\frac{2(x-1) + 3(y-1)}{\varepsilon}\right)$$

is the exact solution of (1). This function has the typical boundary layers at $x = 1$ and $y = 1$, see Fig. 5.

In Table 9 we present the numerical results of the method NSD1 for $\varepsilon = 10^{-6}$, $\delta = 0.25\,h$, and $\sigma_E = 0$ and $\sigma_E = 1$, respectively. The nonconforming SDFEM combines good stability with high accuracy outside the layers. The errors in Table 9 are computed in the subdomain $0 \le x, y \le 0.9$. The convergence rates using the errors on two consecutive grid levels oscillate. For that reason, in Table 9 average convergence rates between level 5 and 7 are given. From Table 9 we see that outside the layers the method without jump terms needs a more refined mesh to achieve the same accuracy as the method with jump terms. An

impression of the errors of the computed solutions inside the layers gives Fig. 6. Similar to Example 2 the error oscillates heavily if the method without jump terms is applied.

References

1. Adams, R.A. (1975): Sobolev Spaces. Academic Press, New York San Francisco London
2. Clément, P. (1975): Approximation by finite element functions using local regularization. RAIRO Anal. Numér. **9**, 77–84
3. Crouzeix, M., Raviart, P.A. (1973): Conforming and nonconforming finite element methods for solving the stationary Stokes equations. RAIRO Numer. Anal. **3**, 33–76
4. Dorok, O. (1995): Eine stabilisierte finite Elemente Methode zur Lösung der Boussinesq-Approximation der Navier-Stokes-Gleichungen. PhD thesis, Otto-von-Guericke-Universität Magdeburg
5. Dorok, O., Grambow, W., Tobiska, L. (1994): Aspects of the finite element discretizations for solving the Boussinesq approximation of the Navier-Stokes equations. In: Hebeker, F.-K., Rannacher, R., Wittum, W. (eds) Numerical methods for the Navier–Stokes equations. Proceedings of the International Workshop on Numerical Methods for the Navier-Stokes equations held at Heidelberg Oct 25-28, pages 50–61. Vieweg-Verlag
6. Dorok, O., John, V., Risch, U., Schieweck, F., Tobiska, L. (1996): Parallel finite element methods for the incompressible Navier–Stokes equations. In: Hirschel, E.H. (ed.) Flow Simulation with High-Performance Computers II. Vieweg-Verlag, Notes on Numerical Fluid Mechanics, vol. 52, pages 20–33
7. Eriksson, K., Johnson, C. (1993): Adaptive streamline diffusion finite element methods for stationary convection-diffusion problems. Math. Comp. **60**, 167–188
8. Hughes, T.J.R., Brooks, A.N. (1979): A Multidimensional Upwind Scheme with no Crosswind Diffusion, volume 34 of AMD. ASME, New York
9. Johnson, C., Saranen, J. (1986): Streamline diffusion methods for the incompressible Euler and Navier–Stokes equations. Math. Comp. **47**, 1–18
10. Johnson, C., Schatz, A.H., Wahlbin, L.B. (1987): Crosswind smear and pointwise errors in the streamline diffusion finite element methods. Math. Comp. **49**(179), 25–38
11. Layton, W., Maubach, J., Rabier, P. (1995): Robustness of an elementwise parallel finite element method for convection-diffusion problems. Technical report, ICMA-93-185 Department of Mathematics and Statistics University of Pittsburgh
12. Lube, G., Tobiska, L. (1990): A nonconforming finite element method of streamline-diffusion type for the incompressible Navier-Stokes equations. J. Comp. Math. **8**(2):147–158
13. Maubach, J., Rabier, P. (1995): Nonconforming higher order polynomial degree elements of Crouzeix-Raviart type for a parallel finite element method. Technical report, Department of Mathematics and Statistics University of Pittsburgh
14. Nävert, U. (1982): A finite element method for convection-diffusion problems. PhD thesis, Chalmers University of Technology Göteborg
15. Niijima, K. (1990): Pointwise error estimates for a streamline diffusion finite element scheme. Numer. Math. **56**, 707–719
16. Ciarlet, P.G. (1991): Basic error estimates for elliptic problems. In: Ciarlet, P.G., Lions, J.L. (eds) Handbook of Numerical Analysis, volume II, pages 19–351. North-Holland Publishing Company Amsterdam New York Oxford Tokyo
17. Risch, U. (1990): An upwind finite element method for singularly perturbed elliptic problems and local estimates in the L^∞-norm. Math. Modél. Anal. Numér. **24**(2), 235–264

18. Roos, H.-G., Stynes, M., Tobiska, L. (1996): Numerical Methods for Singularly Perturbed Differential Equations. Convection-Diffusion and Flow Problems. Springer-Verlag
19. Schieweck, F., Tobiska, L. (1989): A nonconforming finite element method of upstream type applied to the stationary Navier-Stokes equations. RAIRO Numer. Anal. **23**, 627–647
20. Schieweck, F., Tobiska, L. (1996): An optimal order error estimate for an upwind discretization of the Navier–Stokes equations. Numer. Methods Partial Different. Equations, to appear
21. Tobiska, L. (1993): Stabilized finite element methods for the Navier-Stokes problem. In: Miller, J.J.H. (ed.) Applications of Advanced Computational Methods for Boundary and Interior Layers, pages 173–191. Boole Press, Dublin
22. Tobiska, L., Verfürth, R. (1996): Analysis of a streamline diffusion finite element method for the Stokes and Navier–Stokes equations. SIAM J. Numer. Anal. **33**(1), 107–127
23. Wittum, G. (1989): On the robustness of ILU–smoothing. SIAM J. Sci. Stat. Comput. **10**, 699–717
24. Zhou, G. (1995): How accurate is the streamline diffusion finite element method? Math. Comp. **66**, 31–44

This article was processed by the author using the LaTeX style file *pljour1m* from Springer-Verlag.